

# Developmental precise excision of *Oxytricha trifallax* telomere-bearing elements and formation of circles closed by a copy of the flanking target duplication

Kevin Williams, Thomas G. Doak and Glenn Herrick<sup>1</sup>

Department of Cellular, Viral and Molecular Biology, University of Utah School of Medicine, Salt Lake City, UT 84132, USA

<sup>1</sup>Corresponding author

Communicated by A. Toussaint

**The 4.1 kbp TBE1 elements of *Oxytricha fallax* and *Oxytricha trifallax* are deduced to transpose into a centric-symmetric target, CAN<sub>T</sub>G, and to duplicate the central AnT. Despite conserved C(A<sub>4</sub>C<sub>4</sub>)<sub>2</sub> telomeric repeats at their tips, free TBE1s found during macronuclear development are not linear but 4.1 kbp circles closed on one copy of the AnT target duplication. The macronucleus-destined flanks are rejoined to regenerate the target, effecting efficient and precise somatic reversion of the germline transpositional mutation. A model is presented in which transposase catalyzes concerted precise rejoining of the flanks and cyclization of the excised element.**

**Key words:** ciliated protozoa/developmental genome rearrangements/TBE1/transposon

## Introduction

The telomere-bearing elements, or TBE1s, have been identified in *Oxytricha fallax* and *Oxytricha trifallax*, closely related hypotrichous ciliated protozoans (Herrick *et al.*, 1985; Hunter *et al.*, 1989). Several features indicate TBE1s are transposons. TBE1 numbers per host genome are large and vary from isolate to isolate. Comparison of TBE1-interrupted and -uninterrupted alleles suggests that TBE1s cause target duplications (3 bp) upon insertion and have inverted terminal repeats (ITRs). The ITRs are 78 bp long and the distal 17 bp are *Oxytricha* telomere repeats: G<sub>4</sub>T<sub>4</sub>G<sub>4</sub>T<sub>4</sub>G<sub>1</sub> (Herrick *et al.*, 1985). TBE1s are large enough (~4.1 kbp) to encode several proteins.

In ciliate conjugation meiotic products of the two parental micronuclei (MICs) fuse to form a zygotic nucleus. Mitoses then generate new MICs and a precursor or anlage of the new macronucleus (MAC), while the old MAC is resorbed. During anlage development, especially in hypotrichous ciliates, massive genome reorganization occurs, leading to a MAC with gene-sized chromosomes and lacking >95% of the germline sequences (for reviews see Yao, 1989; Klobutcher and Jahn, 1991; Prescott, 1992; Herrick, 1993). Following or during a period of chromosome polytenization, internal eliminated sequences (IESs) are deleted; each that is bounded by short direct repeats, suggesting that IESs are derived from transposons (reviewed by Klobutcher and Jahn, 1991). While most known IESs are small and not detectably repetitive, large repetitive transposon-like elements also are eliminated as IESs; these include *Oxytricha*

TBE1s and *Euplotes crassus* Tec elements (see Klobutcher and Jahn, 1991). One of the two short direct repeats flanking each IES also is eliminated; in transposon terms, this is 'precise excision' and rejoins the flanks to regenerate the pre-transposition target. Because genes are only expressed in the MAC (reviewed by Herrick, 1993), transpositions are phenotypically silent, yet the elements are transmitted through the silent germline MIC. Given a situation so favorable to propagation, it is not surprising that thousands of TBE1s can exist in the MIC (Herrick *et al.*, 1985).

Previous studies of TBE1 excision (Herrick *et al.*, 1985; Hunter *et al.*, 1989) were necessarily indirect, due to *O. fallax* infertility. Here we describe TBE1 excision during the ~4 day developmental processes following conjugation of fertile *O. trifallax* strains. Excision has been monitored by characterizing the immediate precursors—parental MIC loci carrying TBE1s—and products, the MAC-destined TBE1 flanks and the excised TBE1s. Circles of *E. crassus* Tec elements and small IESs are observed concomitant with excision (see Klobutcher and Jahn, 1991). Both kinds of circles are joined by a novel heteroduplex structure (Jaraczewski and Jahn, 1993; Klobutcher *et al.*, 1993). Because the TBE1 elements bear telomeric repeats at their ends, we suspected excised TBE1s might be linear. Instead, we report TBE1 circles in MAC development, but the circle junction differs from that of the *E. crassus* cases: analysis of target sequences indicates TBE1 circles carry away a homoduplex copy of the target duplication. A model is discussed in which transposase cyclizes the excised TBE1 and precisely rejoins its MAC-destined flanks in a coupled reaction.

## Results

### TBE1s in *O. fallax* and *O. trifallax*

Previous work characterized TBE1s in *O. fallax* (Herrick *et al.*, 1985; Hunter *et al.*, 1989). TBE1s initially were detected in *O. trifallax* by DNA hybridization (Hunter *et al.*, 1989). Here we further describe TBE1s in two cross-fertile isolates of *O. trifallax*, each with ~10<sup>3</sup> TBE1s per cell (G. Herrick, unpublished). TBE1s in the two species are very similar, but elements within a species are more similar to each other than to elements between species (K. Williams, A. Seegmiller, T. G. Doak and G. Herrick, in preparation; see below). Therefore, TBE1s of *O. fallax* and *O. trifallax* are designated TBE1-fal and TBE1-tri, respectively. TBE1s are numbered in the order of discovery: the first two found in *O. fallax* are named TBE1-fal-1 and TBE1-fal-2, or fal-1 and fal-2, and the first TBE1-tri element found in *O. trifallax* is tri-1.

### TBE1-tri-1 isolation and characterization

TBE1-fal-1 and -fal-2 are neighboring interruptions in the MIC vC allele of the gene encoding a homolog of mito-

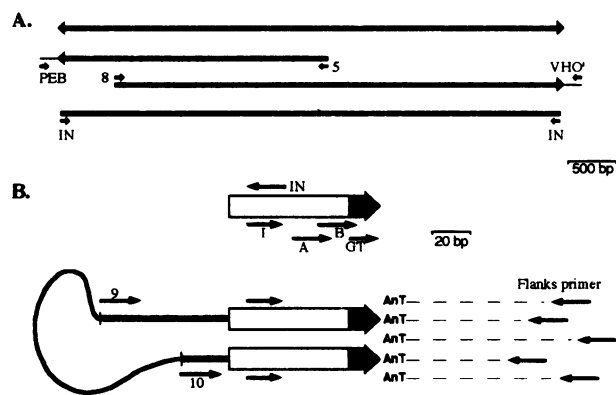


**Fig. 1.** Strategies for PCR amplification of TBE1-tri DNAs. (A) Amplification of TBE1-tri-1 from JRB310 MIC DNA. Thick lines represent the body of the element and the terminal arrows represent its ITRs; thin lines represent MAC-destined flanks. Short arrows represent PCR primers. Except for the ITR and primer symbols, sizes are drawn to scale. TBE1-tri-1 was amplified from MIC DNA in two parts, from each flank across its center, so that the two products overlap by 1.7 kbp; products were produced using primers PEB and 5 (2.31 kbp) and VHO' and 8 (3.76 kbp). The success of these reactions is one indication that tri-1 is inserted in the JRB310 81-MAC region in the opposite orientation to that of fal-1 and -2 in the *O. fallax* vC MIC allele. The bottom line indicates a ~3.9 kbp tri-1 amplification product, from one ITR to the other, generated with the primer 'IN', and a mixture of the overlapping 2.31 and 3.76 kbp primary PCR products as template. (B) Amplification of collections of TBE1-tri ends and flanks. A canonical tri ITR is shown first, drawn to scale; the black section represents the terminal telomeric repeats; primers are indicated as thin arrows. Below is the canonical tri map, with the two ITRs and adjacent sequences juxtaposed and the bulk of the map shrunk (thin curve). See Results and Materials and methods for explanation. Many unrelated flank products are expected in a reaction primed with a given 'Flanks' primer and a TBE1 primer (9,10 or I). At the right the several dashed lines terminating with the 'Flanks' primer arrow represent the collection of products; all align at the left, including the ITR and the target sequence, 'AnT'. Note that a reaction primed with a 'Flanks' primer and the ITR primer I should produce a collection in which some flanks are adjacent to the primer 9 end and others are adjacent to the primer 10 end. In contrast, the collection produced with a 'Flanks' primer and primer 10 should represent only flanks adjacent to element 10 ends.

chondrial solute carriers (HMSC); the elements interrupt the HMSC open reading frame, which is transcribed from MAC DNA after their removal (Herrick *et al.*, 1985; Hunter *et al.*, 1989; Williams and Herrick, 1991). In *O. trifallax* JRB310 DNA we once again find a TBE1 interrupting an HMSC MIC allele. Surprisingly, this element, tri-1, sits only 6 bp from where fal-2 sits in the *O. fallax* vC allele (Figure 2, below), but in the opposite orientation. It also interrupts the HMSC open reading frame.

MIC DNA including tri-1 was PCR-amplified from whole-cell JRB310 DNA (Figure 1A). Two overlapping segments were generated, each from a MAC-destined flank, across the tri-1 center. Portions of the overlapping regions of the two products were sequenced in parallel with corresponding portions of a PCR product representing a mixture of most tri family members. The two tri-1 products are identical in the regions sequenced (534 of 534 bp, unpublished) and differ from the family mixture at 11 positions, indicating tri-1 is a single family member. Its ITRs and flanks were sequenced (see Figures 2 and 3A), identifying the insertion point in the HMSC gene and allowing a size of 4.1 kbp to be calculated.

The sequenced portions of tri-1 differ from the homo-

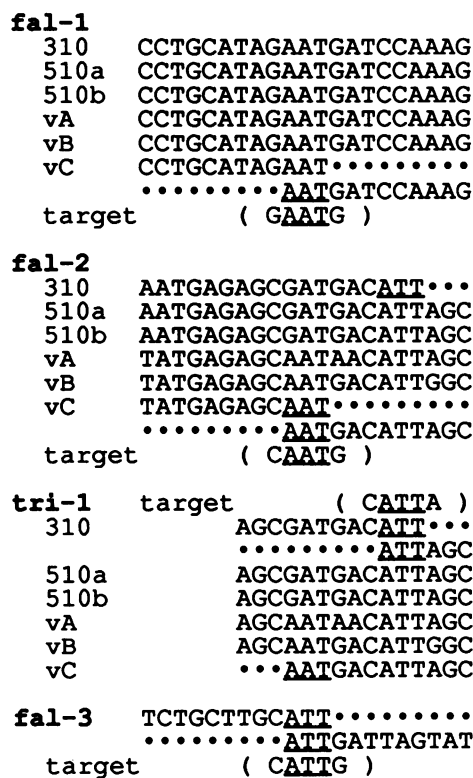


**Fig. 2.** Insertion sites of four TBE1s, sequences of corresponding 'empty' alleles and deduction of target sites. The sequences interrupted by each of the four elements are shown and the sequences of the TBE1s are represented as dots; these same sequences also are presented more fully in Figure 3. The 3 bp direct repeat flanking an element is underlined and the two copies are aligned in consecutive lines to indicate the duplication. The first three TBE1s (fal-1, fal-2 and tri-1) each interrupt an allele of the HMSC gene. The MIC DNA sequences of the uninterrupted 'empty' alleles are shown in register with the TBE1-bearing allele; fal-1 and -2 interrupt the *O. fallax* vC HMSC allele, whereas tri-1 interrupts the *O. trifallax* 310 allele. The display for tri-1 is shifted six positions to the right, so that its sequences align with those of the fal-2 display, indicating the insertion points of the two elements lie only 6 bp apart in their respective alleles. Target site sequences deduced to exist at the time of transposition of each element are presented in parentheses.

logous sequences of fal-1 (F.P.Doerder and G.Herrick, in preparation) at 36 positions (93% identity), giving one indication of the similarity between the fal and tri families. The tri-1 termini are identical 78 bp inverted repeats; they are 88% identical to fal ITRs, including the characteristic 17 bp of telomeric repeat DNA at the ITR end, and differ from fal ITRs at nine positions in a central region (Figure 3, below).

#### Canonical 4.1 kbp TBE1 size

Nearly the full lengths of five TBE1s have been PCR-amplified. A single PCR primer was used that primes inwards from each ITR across the element ('IN,' Figure 1A). The lengths of four cloned fal elements were analyzed, including fal-1 and fal-2, and two further fal elements, fal-3 and fal-4. The four IN-to-IN PCR products exactly comigrate, with a size of ~3.9 kbp (D.Wall, F.P.Doerder and G.Herrick, unpublished). The IN-to-IN reaction also produces a single product of exactly the same size, when a mixture of the two PCR products carrying the overlapping tri-1 segments is used as template (not shown). Thus, tri-1

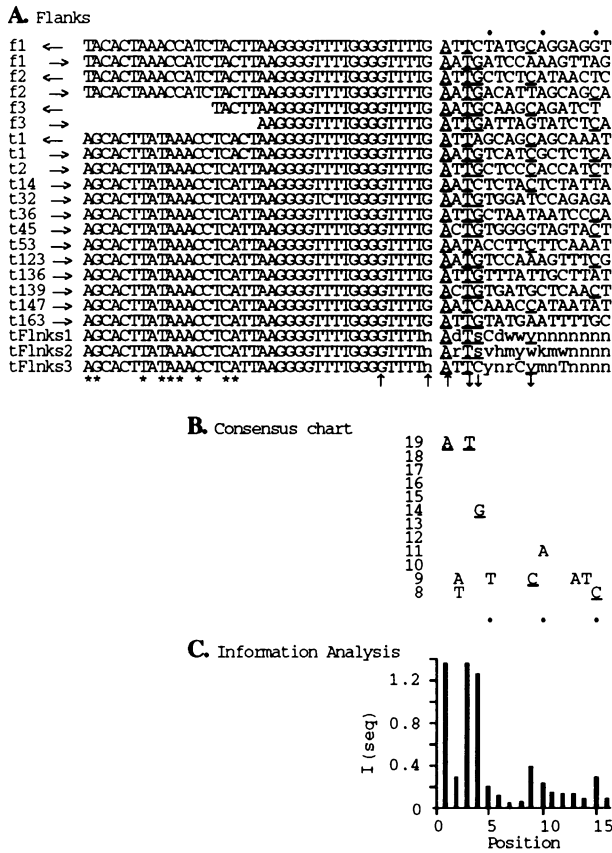


**Fig. 3.** TBE1 termini and flanking sequences. (A) Alignment of DNA sequences of 19 individual TBE1 ends and their adjacent flanks (name abbreviations: fl and tl mean fal-1 and tri-1, respectively), followed by sequences of three collections of ends and their aggregate flanking sequences ('tFlnks'). Horizontal arrows indicate for a given end that it is adjacent to the binding site for primer 9 (←) or 10 (→; see Figure 1A). Ambiguity codes for flanks: s = C,G; w = A,T; y = C,T; r = G,A; k = G,T; d = A,G,T; v = G,A,C; n = G,A,T,C. Dots above the flank sequences indicate positions 5, 10 and 15. Below the alignment, an asterisk indicates differences between TBE1-fal and -tri sequences. Vertical arrows mark symmetric features centered both around insertion points and element-flank junctions. (B) Flank sequence consensus chart. Only the 19 individual flank sequences shown in panel A are represented. For each position, the frequency of the most frequent nucleotide(s) is indicated. (C) Information content analysis. The  $I_{(seq)}$  value for each position of the flank alignment was calculated (Goodrich *et al.*, 1990) as the sum of  $I_b$  for each base, where  $I_b = f_b \log_2(f_b/p_b)$  and  $f_b$  is the frequency of base b (where  $f_b = 0$ , then  $I_b = 0$ ).  $p_b$  is the total frequency of each base b, averaged across the 11 flank sequences (full sequences not shown) and for fal-1, fal-2 and tri-1 across the HMSC codons (Williams and Herrick, 1991) ( $pG = 0.17$   $pA = 0.33$   $pT = 0.33$   $pC = 0.17$ ). For positions where  $I_{(seq)} > 0.25$ , the dominant nucleotide is underlined in panels A and B.

is indistinguishable in size from all four characterized fal elements. The full sequence of fal-1 is 4073 bp long (F.P.Doerder and G.Herrick, in preparation), indicating that 4.1 kbp is the canonical size for TBE1 elements. Southern blots of restricted *O.fallax* and *O.trifallax* DNAs support the conclusion that most TBE1s are the same size and share many restriction sites (Herrick *et al.*, 1985; unpublished). PCR reactions templated with whole-cell DNAs, and primed with various pairs of internal TBE1 primers, produce homogeneous-length products representing most family members (K.Williams, A.Seegmiller, T.G.Doak and G.Herrick, in preparation). Together these results show most TBE1s are ~4.1 kbp long.

### Specific centri-symmetric transposition target

Four out of four TBE1s examined are bounded by short 3 bp direct repeats that we interpret as target site duplications created during transposition (Figure 2). In three cases, five further alleles of the uninserted target are known, in each case lacking the element and one flanking repeat (Figure 2). Further, in each case the duplicated sequence has been fully conserved in all six alleles; thus, AAT or ATT was the sequence present at the time of insertion (Figure 2). No 'empty' alleles corresponding to the fal-3 locus have been characterized, but its sequence is fully consistent with duplication of AGT upon fal-3 insertion. Thus, all four elements seem to share a specificity for insertion into the centri-symmetric sequence AnT, degenerate at the center.

Because the target is centri-symmetric, by one interpretation only the central nucleotide is duplicated, in which case the TBE1 ITR would be 1 bp longer, TCA<sub>4</sub>...T<sub>4</sub>GA (Herrick *et al.*, 1985). We favor the 3 bp duplication interpretation, in part because then the element terminates with the telomere sequence, CA<sub>4</sub>...T<sub>4</sub>G. Such ambiguity exists for the Tec elements and small IESs of the related hypotrichous ciliate *E.crassus* and for *Caenorhabditis elegans* Tc1; each of these elements is either flanked by a TA duplication or is 2 bp longer with no duplication (Rosenzweig *et al.*, 1983; Klobutcher and Jahn, 1991). IS630, to which TBE1, the Tecs and Tc1 are related (Henikoff, 1992; Doak *et al.*, 1993), has been proved to duplicate the TA of its target (Tenzen *et al.*, 1990).

To determine whether TBE1s are usually flanked by AnT, we devised a PCR strategy to obtain collections of flanks. A TBE1 primer directed 'off shore', such as 9, 10 or I (Figure 1B), was coupled with an unrelated primer. We expected such a primer—designated a 'Flanks' primer—might fortuitously match flanking sequences within amplifiable distances of a small subset of the few thousand TBE1 ends in DNA MIC (Figure 1B). Four such sets of heterogeneous PCR products were made, primed with different 'Flanks' primers. Nested PCR tests indicated that such a reaction produces primarily a collection of TBE1 flanks (see Materials and methods), as subsequent analyses bear out. Sequencing three of these collections gave gels that were easily readable through the ITR sequence, indicating their tight conservation ('tFlnks', Figure 3A). A few further nucleotides also were readable, into the collection of TBE1 flanks; further positions were fully ambiguous, as expected (Figure 3A). Flank positions 1 and 3 are unambiguously A and T, respectively. Flanks from the fourth PCR collection were cloned and 11 were sequenced (tri-2 through tri-163, Figure 3). In each case, positions 1 and 3 again are A and T. A consensus table of flank sequences (Figure 3B) shows positions 1 and 3 are always A and T; we refer to these invariant flanking positions as 'A1' and 'T3'. Information content analysis (Figure 3C) confirms that A1 and T3 are not predicted solely by biased base composition and indicates high specificity for these centri-symmetric sites in the target.

Position 2 is degenerate: while many flanks show A2 or T2, collections 1 and 2 show some frequency of G2, and tri-45 and tri-139 have C2 (Figure 3A). Information content analysis (Figure 3C) fails to support any bias at position 2 beyond that imposed by AT richness of the flanking sequences. Thus the consensus target repeat sequence is AnT, which is centri-symmetric. For fal-2 and fal-3 there are two further flanking symmetric positions: C AnT G.

Consensus and information content analyses (Figures 3B and C) strongly support this impression, showing that G4 is frequent and implying that TBE1 elements often transpose into the 5 bp centri-symmetric target CAnTG, as did *fal-2* and (presumably) *fal-3*. However, perfect CAnTG targets were not used for the insertion of *fal-1* (gAaTG) or *tri-1* (CArTa) (Figure 2). Thus, targets with extended centri-symmetric character are preferred, but degenerate targets also are used. Transposon *Tn10* acts analogously, with specificity for a degenerate 7 bp centri-symmetric target with a fully degenerate center base pair, GCTnAGC (Bender and Kleckner, 1992).

*Tn10* target sequences outside the 7 bp core also play a major role in specificity (Bender and Kleckner, 1992). In TBE1 flanks, information content analysis suggests that outside CAnTG, C9 and C15 might contribute to specificity (Figure 3C). During excision a symmetric dimer of transposase might bind to one ITR-flank junction, centered on the target duplication (see Discussion). The dimer could often contact flank bases 4 and 9 and the symmetrically disposed bases on the other strand of the ITR, which are Gs (Figure 3A, bottom line): flank C9 is frequent and C4 is tolerated. Also, ITR-flank junctions are potential targets, with the nearly symmetric form: G.....gAaTG.....C (Figure 3A).

#### Precise excision of *tri-1*

Analyses of *O. fallax* MAC DNA demonstrated precise excision of *fal-1* and *fal-2*, which presumably occurred during MAC development; in MAC DNA the HMSC coding region lacks each entire TBE1 and one of its flanking direct 3 bp repeats (Hunter *et al.*, 1989).

To monitor precise excision, we mated JRB310, to in effect introduce *tri-1* into the developing MACs of progeny, and we followed the fate of the *tri-1* flanking sequences. With PCR and sequencing we first determined the HMSC genotypes of JRB310 and its partner, JRB510; PCR then allowed quick genotyping of progeny (K. Williams, T.G. Doak, A. Seegmiller, T. Messick and G. Herrick, in preparation). JRB310 is homozygous for the *tri-1* bearing allele '310', whereas JRB510 is heterozygous, carrying two further alleles, '510a' and '510b', neither of which bears a TBE1.

To analyze exconjugants inheriting *tri-1*, we mated JRB310 and JRB510 cells and cloned exconjugants that showed overt and persistent MAC anlagen. Fourteen F1 lines were identified that received the 310 allele from JRB310 and hence processed *tri-1* during the development of their MAC anlagen. The MAC HMSC DNAs of each of the 14 lines were analyzed by PCR and direct sequencing to learn the fate of the *tri-1* flanks.

The result for one of those clones, 'SLC32', is shown in Figure 4C. The sequence of the 310 MAC product is identical in the excision region to JRB510 MAC DNA (Figure 4A), which was derived from MIC alleles lacking *tri-1*. Hence, *tri-1* and one flanking repeat (AAT on the strand sequenced, ATT as shown in Figure 2) have been eliminated, exactly reverting the germline HMSC mutation created by *tri-1* insertion. Parallel analyses of the remainder of the 14 F1 lines showed that *tri-1* precise excision had occurred in each episode of MAC development. Thus, *tri-1* excision is regularly precise.

The exconjugant line SLC32, like three others, is special, having the same homozygous 310 genotype as JRB310. In

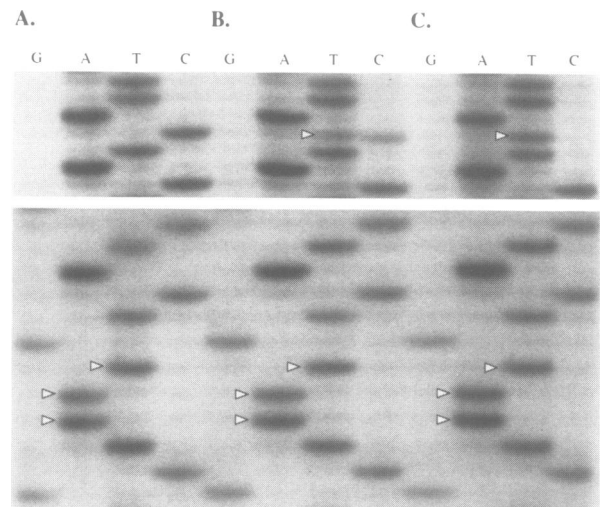


**Fig. 4.** Precise excision of TBE1-*tri-1*. Sequencing from primer 1457- was performed on bulk PCR products amplified from MAC DNAs with primers bracketing the *tri-1* excision site (PEB and VHO'). Upper and lower panels show portions of a sequencing gel autoradiogram. The lower panel indicates the region of *tri-1* excision or the corresponding empty site; the marked AAT (arrows) represents the sequence duplicated by *tri-1* insertion in MIC DNA (see Figure 2, where sequence of opposite strand is shown). The upper panel indicates a dimorphic position (arrows) further from primer 1457-, in intron 2 of the HMSC gene; alleles 510a and 510b have a C, while allele 310 has a T. (A and C) The PCR templates were 10 cell equivalents of whole-cell DNAs purified from, respectively, JRB510 (alleles 510a + 510b) and a uniparental JRB310 progeny line SLC23 (310 homozygote). (B) Ten emerging exconjugants from a mating of JRB310 and JRB510 were lysed directly in the PCR reaction.

these uniparental cases MAC development and *tri-1* precise excision occurred in the absence of an 'empty' allele (see Discussion). [Besides the four 310 + 310 uniparental progeny, two 510a + 510b progeny also were found, as were 10 typical biparental progeny, in the expected Mendelian ratio, five 310 + 510a and five 310 + 510b. Uniparental progeny are observed in a variety of different ciliates and can arise in at least three different ways: selfing, cytogamy or autogamy (Grell, 1973).]

In the F1 DNAs no sequence heterogeneity was detected at or beyond (above) the target site, and thus there was no evidence for imprecise excision (Figure 4C versus A), even though the full mixture of PCR products was directly sequenced. However, imprecise excisions still might be common (discussed by Hunter *et al.*, 1989): first, multiple chromatids of the TBE1-bearing locus may be generated during polytenization before excisions occur (see below) and second, *fal-1*, *fal-2* and *tri-1* interrupt the HMSC coding region. Thus, imprecise excision products might have been generated in the anlage, but selection for HMSC function during subsequent clonal growth could have caused biased retention of precise products, explaining our results analyzing MAC DNA from clonally propagated cells.

To assess the fidelity of *tri-1* excision, its flanks were examined directly in JRB310 × JRB510 exconjugants, before any exconjugant growth occurred. Individual exconjugants were hand picked, as above, and later harvested for PCR as they resumed the vegetative form (3–4 days after pairing), but before they grew or divided. (This stage occurs ~1 day after the old MAC already has been resorbed and no old MAC DNA was detected by PCR; unpublished con-

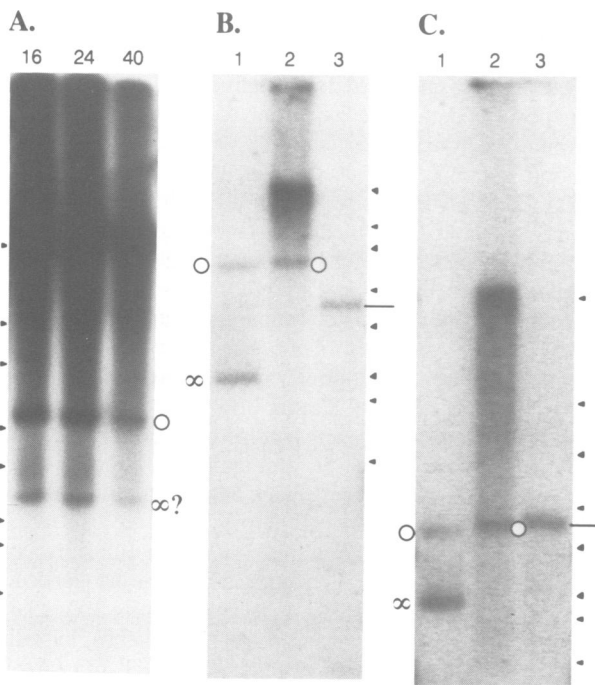


**Fig. 5.** TBE1 circles in exconjugant DNA. Autoradiograms of agarose gel blots hybridized with an internal 1.3 kbp section of *fal-2*. (A) Blot from 0.7% agarose gel, each lane with DNA from  $\sim 1.5 \times 10^4$  cells, harvested after maximal pairing at the times indicated (h). Bands marked:  $\circ$ , open circles;  $\infty?$ , probable supercoils (not detected in subsequent experiments, where we suspect supercoils suffered artifactual nicking). (B and C) Blots from 0.5 and 1.3% agarose gels. Lanes B2 and C2 carry exconjugant DNA from  $\sim 8 \times 10^3$  cells; TBE1 band ( $\circ$ ) is indicated by open circles. Outside lanes carry 30 ng of a variously treated 4.0 kbp plasmid (probe contained a trace of the plasmid). Plasmid bands:  $\infty$ ,  $\circ$ , 4.0 kbp supercoils and X-ray nicked circles in lanes B1, C1; —, 30 ng of linear DNA in lanes B3 and C3. Limit-mobility TBE1 material seen in these blots in large part could be derived from MIC DNA, coming from several sources: in the mating represented in Figure 5B and C, 41% of the cells did not mate and vegetative cells carry an average of 2.4 MICs each; furthermore, each exconjugant with a developing MAC carries two new MICs and early anlagen also are accompanied by lingering post-meiotic and post-zygotic relic nuclei (T.G.Doak, unpublished). Arrows next to each panel represent mobilities of linear size standards (23130, 9416, 6557, 4361, 3236, 2322, 2027 and 1444 bp, in descending order).

trols.) A MAC interval including the *tri-1* excision site was PCR-amplified. To avoid random exclusion of rare product types in a given PCR reaction, nine pools of 10 exconjugants each were directly lysed in PCR reactions. Each of the nine PCR products was directly sequenced, giving essentially identical results. Figure 4B shows sequencing lanes representing one pool. Note the 'T' band marked in the upper panel, showing that the 310 allele is well represented in the 10 pooled new MACs. Again, the sequencing quality in both panels is comparable with that in Figure 4A, representing the homogeneous JRB510 sequence, generated without TBE1 excision. Thus, even before any selection for function of 310 products, there is no evidence for imprecise excision of *tri-1*. We feel confident that at least most *tri-1* excisions give precise somatic reversion products. Tausta *et al.* (1991) drew the same conclusion regarding *E. crassus* IES and *Tec1* excision.

High efficiency of *tri-1* precise excision also is indicated by the yield of products, because the ratio of precise excision

products to unaltered 510a + b products is  $\sim 1:1$  (intensities of marked 'T' and 'C' bands in Figure 4B), comparable with the expected input ratio of 310 and 510a + b chromatids. These results also establish that *tri-1* excision occurs during MAC development.

#### Free 4.1 kbp TBE1 circles in exconjugants

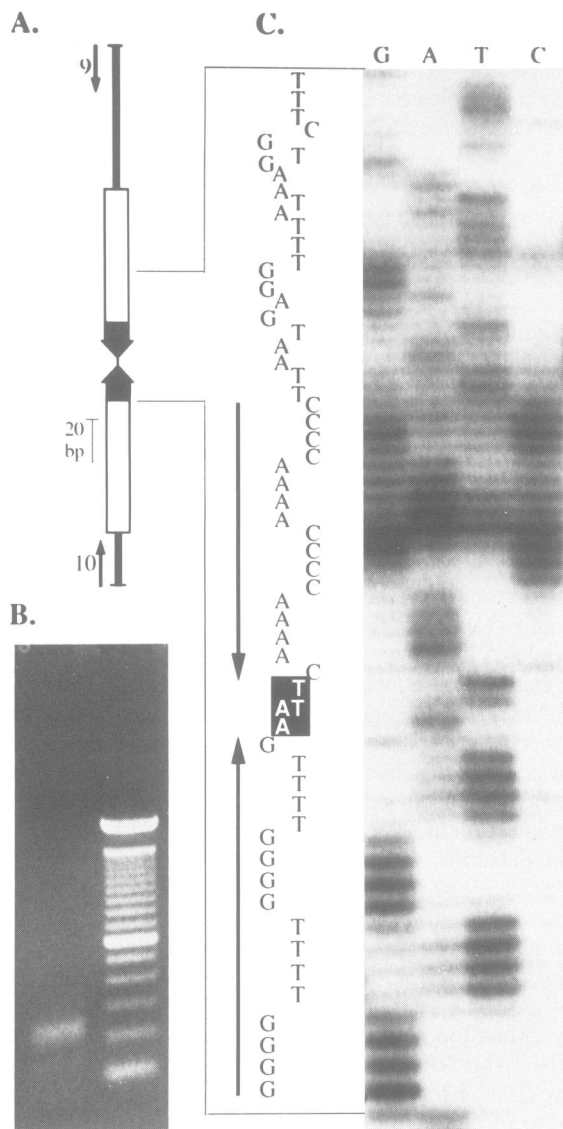
Not only is *tri-1* absent from MAC DNA, but indeed all of the  $\sim 10^3$  TBE1s in *O. trifallax* JRB310 or 510 are absent from MAC DNA (not shown), as shown previously for TBE1s of *O. fallax* (Herrick *et al.*, 1985). This implies massive elimination of TBE1s during MAC development. To look for TBE1s excised during MAC development, large matings between JRB310 and JRB510 were conducted. Exconjugants were harvested  $\sim 16$ , 24 and 40 h after maximal pairing; at these times most exconjugants have distinctly visible developing MACs (not shown). Native whole-cell DNAs were prepared and analyzed on TBE1-probed Southern blots. Because the canonical TBE1 length is 4.1 kbp, we anticipated free 4.1 kbp TBE1s, presumably excised from the developing MACs.

Figure 5A shows two free TBE1 forms. We suspect the faster band is supercoiled 4.1 kbp circles; it has not been seen in subsequent DNA preparations (see Figure 5 legend). In no case have we seen free linear TBE1s and no free forms are seen in vegetative cell DNA (not shown). The slower band consists of nicked  $\sim 4.1$  kbp circles: Figure 5B and C shows blots from gels of differing agarose concentrations; the population of TBE1 DNAs migrates as a band (lanes 2), slightly behind the nicked circle band of a 4.0 kbp *Escherichia coli* plasmid in both gels (lanes 1) and does not migrate with either 4.0 kbp linear (lanes 3) or supercoiled plasmids (lanes 1). In a gel run in sufficient ethidium bromide to just relax plasmid closed circles (not shown), the TBE1 band did not change mobility and again migrated slightly slower than the nicked plasmid. Thus, we find canonical-sized 4.1 kbp TBE1 circles, probably nicked during isolation. Their circular topology is confirmed below by the demonstration of end-to-end junctions.

Most exconjugant TBE1 DNA is not in the circle fraction, but has a limited mobility (Figure 5B and C). Much of this limit-mobility DNA must be derived from MICs, which have a full complement of integrated TBE1s (Figure 5 legend), and some of it may be as yet unexcised TBE1s in anlage DNA. Comparison of blot lanes of vegetative whole-cell DNAs and whole-cell exconjugant DNA (not shown) leads us to suspect that some polytenization has occurred in the developing MACs, amplifying TBE1s that have not yet been excised. In *E. crassus*, *Tec* elements are excised before anlage polytenization, but small IESs are excised much later and yet appear to be excised by the same unique mechanism mediating *Tec* element excision (see Klobutcher and Jahn, 1991; Jaraczewski and Jahn, 1993; Klobutcher *et al.*, 1993). We suspect that individual TBE1s are excised at different times in development and then turn over rapidly. Also, some TBE1s may reside in regions of anlage DNA that are eliminated later in development by a mechanism not related to TBE1 excision. In any case, clearly at least a portion of TBE1s form circles, presumably excision products.

#### TBE1 circle junctions

To investigate potential end-to-end junctions in these circles, DNA was isolated from a circle-containing gel plug and used



**Fig. 6.** Circle junctions. (A) Map of the 251 bp circle junctions, showing the head-to-head ITRs (large arrows) tipped with telomeric repeats (solid), and positions of primer binding sites. (B) Circle junction PCR products (primers 9 and 10) run next to a 100 bp ladder on a 1.5% agarose gel in ethidium bromide. (C) Autoradiogram of sequencing gel with products primed with 10 from bulk circle junction PCR template. The interpretation on the left shows the junction of the two head-to-head blocks of 17 bp telomeric repeats (arrows), with three nucleotides between, the center position showing both A and T bands. The interpretation in some regions relies in part on sequencing of individual cloned junctions. Note the unambiguous bands near the top of the figure (long chains).

as template for PCR with primers 9 and 10, which are directed 'off the ends' (Figure 6A). A population of ~250 bp DNAs should be produced, representing head-to-head, double ITR circle junctions. A band of products with the predicted size was obtained (Figure 6B). As expected, it was difficult to devise reaction conditions to amplify a template carrying a 78 bp hairpin. No product was obtained with limit-mobility DNA template (not shown). PCR template dilution tests were performed (not shown), assaying for the ability to produce the circle junction product from circles and in parallel from a cloned circle junction, or to produce an internal TBE1 interval from circles in parallel with cloned

fal-1. These results show that the circle junction PCR products represent the bulk of the native circles.

The product amplified from native circles was directly sequenced to determine its extent of heterogeneity and to examine the junction structure. Again, as with the PCR reaction, obtaining adequate sequencing reactions from these head-to-head structures was quite difficult, despite the use of various conventional methods to sequence such structures. Figure 6C shows the results of sequencing the bulk product from primer 10 with a Taq polymerase thermocycling procedure. It is immediately apparent that there are many strong stops, especially near the upper (primer-distal) telomeric repeat region (similar results were obtained using primer 9; not shown). Similar low grade results were, however, also obtained using a cloned junction (not shown). Thus, the many apparent ambiguities do not indicate primarily sequence heterogeneity but instead the difficulty of sequencing across a large hairpin.

The bulk sequence autoradiogram (Figure 6C) shows two important points. First, as suggested by the sequences of several individual TBE1 ITRs and flanks (Figure 3A), a large fraction of TBE1s share a conserved ITR sequence, including the terminal 17 bp telomeric sequence,  $(G_4T_4)_2G$  (arrows in Figure 6C). Second, at least most junctions carry three extra nucleotides between the two head-to-head 17 bp telomeric sequences; that one can 'read' the sequence near the top of the gel indicates that most junctions carry the same number of nucleotides between that position and the primer and hence that the number of extra nucleotides at the junction must in general be constant. These three extra nucleotides are A, then mostly A or T, then T. While one easily could dismiss the central A/T ambiguity as artifactual, we believe it is real, because AnT is the conserved TBE1 target duplication sequence (Figures 2 and 3A). Thus, excision appears to be conservative, with one copy of the target repeat remaining in the MAC-destined sequence and the other target repeat removed with the TBE1 at its circle junction.

## Discussion

We argue TBE1s are transposons because they strongly resemble demonstrated transposons of the class that transpose directly as DNA (see Introduction). TBE1s might transpose frequently, but we lack the genetic tools traditionally necessary to detect the event. We do show five empty alleles corresponding to each of three TBE1s (Figure 2); conceivably the presence of each element at its respective position is the primitive state, but it seems far more likely that each element has transposed into its site subsequent to divergence of its target from the other five empty alleles. TBE1s interrupt a 5 bp degenerate centri-symmetric site (Figures 2 and 3), which we interpret to be an insertion target site; while such target site specificity is not a universal feature of known transposons, it is not uncommon (e.g. *Tn10* and the *Tc1-IS630* family; see above). Finally, a *fal-1* open reading frame conceptually encodes a 42 kDa basic protein homologous to the transposases of the *Tc1-IS630* family (Doak *et al.*, 1993). These facts constitute strong circumstantial evidence that TBE1 is a transposon that transposes in the MIC directly by a 'cut and paste' mechanism, common to a large variety of transposons (Mizuuchi, 1992), including the *Tc1-IS630* family (Moerman *et al.*, 1991; Plasterk, 1991).

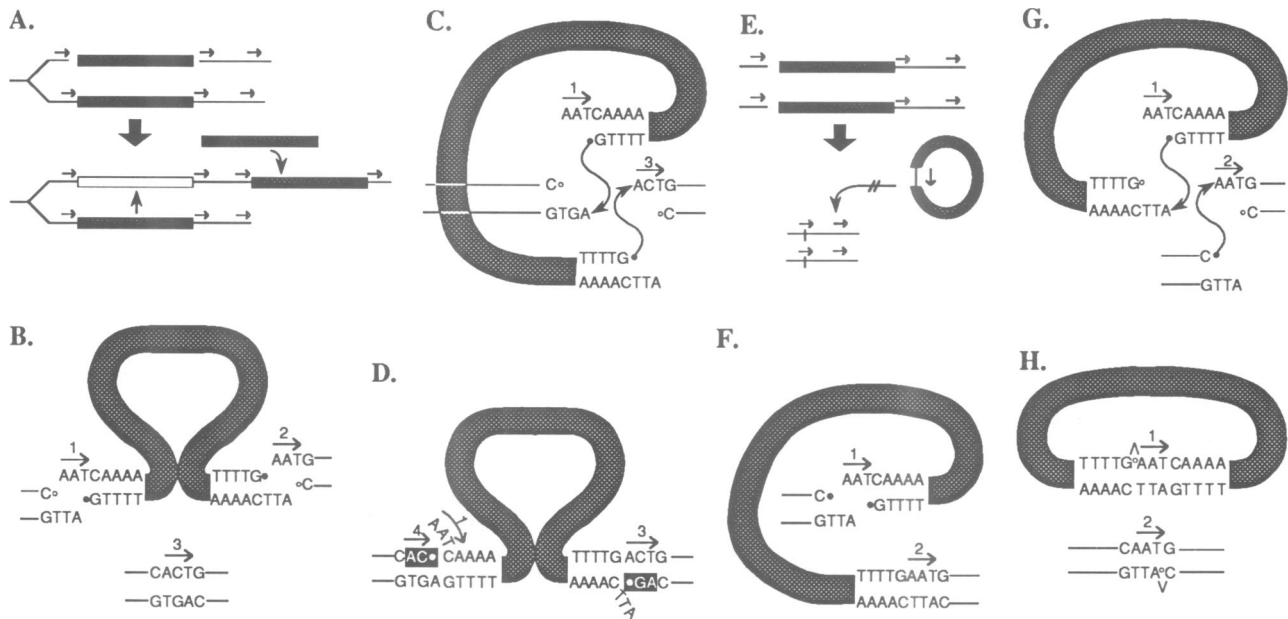


**Fig. 7.** Model relating the mechanisms of TBE1 germline transposition and somatic precise excision. Panels A–D illustrate the currently accepted conservative transposition mechanism (see Mizuuchi, 1992), tailored to TBE1, while panels E–H show a related mechanism proposed for TBE1 precise excision (see text). Thick bars represent TBE1s, thin lines indicate host sequences and short arrows represent 3 bp target duplications. (A) A TBE1 has just been excised from one chromatid soon after the locus was replicated. The excised element transposes to a new site, causing flanking target duplications. Meanwhile the double-strand break at the donor site is repaired from the sister chromatid, creating a replacement (hollow bar) for the transposed TBE1. (B) The TBE1 has been excised from the donor site by staggered double strand cuts at each end, producing 3-nt 5' protrusions that carry one strand each of the target repeats '1' and '2', which were created during the prior transposition. Recessed 3'OH groups are revealed, represented by open and filled circles: filled circles represent 3'OH groups that transposase will activate for the *trans*-esterification step. The new target (below) has the same CAnTG sequence, but a different central nucleotide,  $n = C$ ; in the final step, duplication of the central ACT ('3') will yield a target repeat '4'. (C) During strand transfer the two TBE1 ends and their transposase-activated 3'OH groups displace the target 5' phosphates. (D) Repair synthesis destroys the protruding 5' trinucleotides brought in with the element from the donor target repeats and replaces them (with nucleotides shown against a black background) to create the target duplication at the new target. (E) Two homologs, each carrying the same allele, participate in parallel to give rise to regenerated targets with a single copy of the target duplication and TBE1 circles carrying the other target duplication at the circle junction. Insertion of the excised circles into a new location is blocked. (F) A double-strand break is created at only one TBE1 end; the other end assumes the role of target. Both 3'OH groups bared at the left TBE1 end are activated. (G) Each activated 3'OH group displaces a 3'OH and is joined to a strand at the right end of the TBE1. (H) Target repeat strands pair, leaving two covalent joints, one at the circle junction, the other at the regenerated, MAC-destined target. Host ligation (carets) could seal the remaining 5'P/3'OH nicks.

### The unusual relationship between TBE1 and its ciliate host

Any increase in transposon number is balanced against the negative impact of deleterious mutations on host fitness. TBE1s have attained a very high copy number in *Oxytricha*: the copy number of TBE1s (thousands per MIC) is orders of magnitude higher than that of most transposons (see Berg and Howe, 1989). Apparently, then, TBE1s cause at most modest harm to *Oxytricha*. How has this situation evolved? On the one hand ciliate evolution has created a 'safe haven' for transposons capable of taking advantage of the situation. In particular, hypotrichous ciliates like *Oxytricha* not only do not express genes from the germline MIC, but they delay expression from the MAC anlage until its development is complete (reviewed by Herrick, 1993).

To proliferate freely in the silent germline MIC, TBE1s appear to have refined excision so that germline mutations created by transpositional insertion are fully and cleanly reversed in the developing MAC, with the result that insertion mutations have no phenotype and hence do not directly reduce host fitness. We have described four features of TBE1 excision; each appears to lessen the impact of TBE1 germline transposition by allowing the vegetative MAC to function unimpaired. (i) Excision prior to the onset of MAC gene expression: examination of bulk TBE1s indicates excision has probably begun within the first 2 days of conjugation (when circles appear). Examination of HMSC MAC

products indicates excision of *tri-1* from 310 HMSC chromatids is complete by the end of conjugation (3–4 days; Figure 4B), suggesting that all TBE1s may be eliminated during MAC development. (ii) Efficient excision: the apparently full yield of fully processed 310 allele DNA in mature exconjugants (Figure 4B) indicates that *tri-1* elimination is fully efficient. MAC DNA blot hybridization experiments (TBE1 and HMSC probes) indicate that excision of all TBE1s must be highly efficient (Cartinhour and Herrick, 1984; Hunter *et al.*, 1989; unpublished). (iii) Precise excision: examination of excisions of *fal-1*, *fal-2* and *tri-1* in many independent episodes of MAC development showed only precise somatic reversion of the mutations they cause in the HMSC open reading frame. (iv) Excision as circles. Circular retrotransposon (Goff, 1992) and *IS911* (Polard *et al.*, 1992) DNAs appear to be inert and excised TBE1s appear to form circles, suggesting they cannot transpose into MAC DNA. Taken together, these excision features strongly suggest that TBE1 has been highly successful within the *Oxytricha* germline because it evolved an efficient strategy to avoid impairing host gene expression.

### TBE1 transposition

Below we discuss the possible role of transposase in precise excision. As a prelude, we consider conventional 'cut and paste' transposition (Mizuuchi, 1992), tailored for TBE1 in

the MIC (Figure 7A–D). After a replication fork passes through a TBE1, occasionally transposase excises the element as a free linear DNA by the generation of 3 bp staggered cuts bracketing the target repeats, leaving a double-strand gap in the donor chromatid. The gap is then repaired by the host, often replacing the departed TBE1 with a fresh copy, templated by the intact chromatid (Engels *et al.*, 1990; Moerman *et al.*, 1991; Plasterk, 1991; Hagemann and Craig, 1993). The conserved telomeric repeats at the ends of the liberated element might serve to stabilize it, until its 3'OH termini can attack a target and insert at a new MIC locus (Figure 7C and D). Since TBE1s are absent from the site of vegetative gene expression (the MAC), transposase must be expressed either from the MIC or from the developing MAC, before TBE1 elimination.

#### **Peculiarities of TBE1 precise excision**

Developmental precise excision of TBE1s differs from conventional precise excision. First, conventional excision is rare and usually imprecise (see Berg and Howe, 1989), whereas TBE1 developmental excision apparently is quantitative and always precise. Second, conventional precise excision is a rare outcome of transpositional excision, resulting from host repair of the gap, with an empty-site allele used as the repair template (Engels *et al.*, 1990; Plasterk, 1991; Hagemann and Craig, 1993). In contrast, tri-1 precise excision was demonstrated in JRB310 and four uniparental progeny, despite MIC and anlage homozygosity for the tri-1-bearing allele, and thus in the absence of any empty-site allele to serve as a repair template. [The same must be true for excision of small IESs, which are ancient and probably have routinely gone to fixation, and hence are routinely homozygous (Klobutcher *et al.*, 1984; Herrick *et al.*, 1987; K.R. Williams, T. Messick, A. Seegmiller, T.G. Doak and G. Herrick, in preparation).]

#### **Model for developmental precise excision**

We propose transposase also serves as 'excisase', conducting TBE1 precise excision in the developing MAC. Alternatively, *Oxytricha* might encode excisase. However, because a 'cut and paste' transposase normally conducts excision at the outset of transposition, we propose that transposase is highly expressed during conjugation and below we propose a simple mechanism for transposase-catalyzed TBE1 excision in the developing MAC. Transposase may be differentially transported into the developing MAC, and we imagine it catalyzes transposition in the neighboring MIC only infrequently.

We propose transposase action is altered in the anlage, such that it efficiently produces two products not produced during transposition—precisely rejoined MAC-destined flanks and inert TBE1 circles (Figure 7E–H). In essence, one end of the element transposes into the other, cyclizing the element and regenerating the target. The model shares some features with that proposed by Polard *et al.* (1992) to explain an intriguingly similar—and possibly homologous (Doak *et al.*, 1993)—IS911 reaction catalyzed by high amounts of its transposase. As we see with TBE1s, the IS911 donor is precisely restored, carrying only one copy of the target duplication, and the IS911 is cyclized, carrying the other copy of the target duplication at the circle junction.

In our model, a transposase complex assembles on only one element–flank junction, giving one staggered cut that

brackets the target duplication and generating 3-nt-recessed 3'OH termini (Figure 7F). Then the far element–flank junction is attacked as a target (Figure 7G).

During transposition, a synaptic complex forms, with transposases bound to both ITRs (see Mizuuchi, 1992). In the excision model, only one ITR is bound, but not the second. Instead, the flank adjacent to the first ITR is bound. Transposase affinity for the flank is indicated first by the demonstrated target specificity and second by the assumed affinity for the ITR and the resemblance of the flank to the ITR; recall that the ITR–flank junction is centri-symmetric, G.....gAnTG.....C (Figure 3A). What unusual conditions might foster this flank–transposase interaction in the anlage? (i) Elevated levels of transposase might favor it. (ii) Besides transposase, TBE1 conceptually encodes a protein kinase with two C<sub>2</sub>H<sub>2</sub> zinc fingers (F.P. Doerder and G. Herrick, in preparation); action of DNA-bound kinase might alter a bound transposase monomer, enabling it to bind more tightly to the flank. (iii) During MAC development ~0.7% of dA bases are methylated *de novo* (Rae and Spear, 1978; Cartinhour and Herrick, 1984); methylation of the AnT target duplication might alter its interaction with transposase.

After transposase monomers bind an ITR and its flank, cleavage occurs between them (Figure 7F). Each transposase remains bound and the two new 3'OH groups become activated for strand transfer to the target.

The uncut element–flank junction at the far end should be a good target, being immediately adjacent and having a centri-symmetric target consensus sequence, G.....gAnTG.....C (Figure 3A). The two activated 3'OH groups attack the two target strands (Figure 7G), in a pair of concerted strand transfer reactions exactly analogous to the transposition insertion step (Figure 7C). This concerted step creates both the precisely reverted MAC-destined site and the TBE1 circle, each bearing one of the original target duplications (Figure 7H). The remaining 5'P/3'OH nick on each product might then be sealed by host ligase.

This model is not obviously applicable to precise excision and circle formation by the Tecs and small IESs of *E. crassus*: although the MAC-destined joint does carry one copy of the flanking target duplication, those circles are joined not by a simple copy of the target duplication, but instead by an extensive heteroduplex (Jaraczewski and Jahn, 1993; Klobutcher *et al.*, 1993). Whether this difference between elements in the two ciliates reflects profound underlying mechanistic differences remains to be determined. On the other hand, elimination of the 0.6 kbp M segment in *Tetrahymena* MAC development is formally analogous to the TBE1 reaction. M segment excision generates a MAC-destined junction carrying one copy of the flanking short direct repeat and free circles are detected with a copy at the circle junction (M.-C. Yao, personal communication). M deletion requires two copies of a longer asymmetric sequence, with one copy in each flank, on opposite strands (Godiska and Yao, 1990); in the resulting MAC DNA, the two copies form a split palindrome, reminding us of the centri-symmetric character of the regenerated TBE1 target.

Deletion segments described in *Tetrahymena*, as well as the short IESs described in *Oxytricha* and *Euplotes*, are generally not demonstrably repeated MIC sequences and thus the analogy with transposons seems to break down. Presumably the machinery catalyzing their precise excision is encoded elsewhere in the genome; it may be strictly a host



function, but it is equally possible that the reactions are catalyzed by transposases encoded by families of transposons or transposon relics, as suggested by us and others previously (for a review see Klobutcher and Jahn, 1991).

## Materials and methods

### *O. trifallax* culturing and mating

*O. trifallax* strains JRB310 and JRB510 were chosen for their high copy number of TBE1 sequences ( $\sim 10^3$ /MIC, unpublished) and mating fertility ( $> 70\%$ ). The isolation, description and the details of culturing and mating *O. trifallax* will be described elsewhere (R.L. Hammersmith, K. Williams, T.G. Doak and G. Herrick, in preparation). Matings between JRB310 and 510 are conducted with  $\sim 10^5$  cells in open cultures. Early pairs appear 4–6 h after mixing and maximum pairing ( $> 60\%$ ) occurs within 24 h after mixing.

### DNAs

Whole-cell DNAs were purified as previously described (Dawson and Herrick, 1982). DNAs were purified from agarose gel plugs with Qiaex (Qiagen). TBE1 ITR primers (see Figure 1B): IN (5'-CTTCTGCAGG-AATTTGTAGGGGTTGGG), I (ITR19; Hunter *et al.*, 1989), A (CAAATCAAGCACTTATAAACCT), B (CTTATAAACCTCACTAA-GGGG), GT (GGGGTTTGGGGTTT). TBE1 internal primers 9 (ATCCAAAAGTGCATTTTGGAGTG) and 10 (AGCTTGTAATTTTT-GTCTCGCA) are directed outwards with their 5' ends 142 and 102 bp from the two ends (see Figure 5A). Primer 5 (CCTAATTAAGTACGTAC-CAATTTA) binds  $\sim 1.8$  kbp from the primer 9 site and primer 8 (GAAATGGTATCACTTACAAAGG) binds  $\sim 0.4$  kbp from the primer 10 site (see map, Figure 1A). Other primers: LCR1 (Williams and Herrick, 1991), LCR1' (GTAAAGTAGAGATTTATTTGTTAT), PEA (AACTT-ACGCAGAATAGAATTTCTGGAGTCCA), VHO' (Hunter *et al.*, 1989), PEB (Williams and Herrick, 1991), 1457- (AATAAAATATCGAATCAT-TGATTTTC).

### PCR, sequencing and cloning

PCR reactions (25  $\mu$ l) contained Taq DNA polymerase and provided buffer (Boehringer). Products were isopropanol-precipitated and sequenced directly (GIBCO BRL dsDNA Cycle Sequencing kit), or cloned into a plasmid vector.

The circle junction PCR reaction (35 cycles, 97°C for 15 s, 54°C for 30 s, 72°C for 90 s) contained gel-purified circles ( $\sim 200$  cell equivalents) and primers 9 and 10 (0.2  $\mu$ M each). Flanks PCR reactions (35 cycles, 97°C for 15 s, 56°C for 3 min) contained  $\sim 2$  ng of gel-purified limit-mobility JRB510 DNA, the ITR primer I and a 'flanks' primer, either PEA, PEB or LCR1 (see Results and Figure 1B). Each product had a limited set of heterogeneous-sized DNAs and was sequenced from primer I. A fourth PCR reaction (35 cycles, 97°C for 15 s, 54°C for 3 min) contained  $\sim 2$  ng of limit-mobility JRB310 DNA, primer 10 and the 'flanks' primer LCR1'. The reaction also produced a limited set of heterogeneous-sized products. They were used as template (1  $\mu$ l) in each of four nested secondary reactions. Each nested reaction again used LCR1', coupled with either I, A, B or GT, instead of primer 10. These primers should bind the ITR of bona fide terminal TBE1 products progressively closer to the ITR end (Figure 1B), giving progressively shorter secondary products. Most primary products gave rise to secondary products, shifted to smaller size as expected of flanks; others did not, presumably not flanks. The primary reaction products were treated with T4 DNA polymerase (Dawson and Herrick, 1982) and blunt-end ligated into *Sma*I-cut BSIKS+ (Stratagene), followed by transformation into *E. coli* DH5 $\alpha$  cells. Of 164 insert-bearing clones, 31 carried flank inserts, of which 11 were sequenced from primer 10 (GenBank accession numbers L02852–L02854, L02857–L02864).

DNAs representing MIC sequences from the *O. fallax* vB allele and the *O. trifallax* 310, 510a and 510b alleles were PCR-amplified from whole-cell DNAs using primers specific for MIC-limited sequences (IES-L, IES-R or tri-1). The details of these amplifications and full sequence results will be published elsewhere (K. Williams, T.G. Doak, A. Seegmiller, T. Messick and G. Herrick, in preparation). The sequences have been submitted to GenBank (accession numbers L02855–56 and L020235–39) and relevant segments are presented in Figure 2; vA and vC MIC sequences have accession numbers M13029–30, M13035–42 and N00056.

To perform PCR directly on DNA in individual cells, the cells were hand isolated into water in the PCR reaction tube, lysed with 0.01 N NaOH, brought to pH 8.1 with Tris-HCl, and the full PCR reaction was constituted. Motile cells and cysts both lyse readily; MAC intervals are easily amplified from a single cell;  $> 50$  cells poison the reaction (M. Gillespie, G. Herrick and K. Williams, unpublished).

### TBE1-fal-3 and -fal-4 isolation

Phage  $\lambda$  clones carrying fal-3 and -4 were retrieved by plaque-lift hybridization to a TBE1 probe (A. Lee, D. Wall and G. Herrick, unpublished) from a L47 library of *O. fallax* MIC DNA (Herrick *et al.*, 1985). The two ends and flanks of fal-3 were amplified by inverse PCR and sequenced (F.P. Doerder, S. Christensen, T.G. Doak and G. Herrick, unpublished).

## Acknowledgements

This work was supported by grant GM25203, National Institutes of Health.

## References

- Bender, J. and Kleckner, N. (1992) *Proc. Natl Acad. Sci. USA*, **89**, 7996–8000.
- Berg, D.E. and Howe, M.M. (eds) (1989) *Mobile DNA*. American Society for Microbiology, Washington, DC.
- Cartinhour, S. and Herrick, G. (1984) *Mol. Cell. Biol.*, **4**, 931–938.
- Dawson, D. and Herrick, G. (1982) *Nucleic Acids Res.*, **10**, 2911–2924.
- Doak, T.G., Doerder, F.P., Jahn, C. and Herrick, G. (1993) *Proc. Natl Acad. Sci. USA*, in press.
- Engels, W.R., Johnson-Schlitz, D.M., Eggleston, W.B. and Sved, J. (1990) *Cell*, **62**, 515–525.
- Godiska, R. and Yao, M.-C. (1990) *Cell*, **61**, 1237–1246.
- Goff, S.P. (1992) *Annu. Rev. Genet.*, **26**, 527–544.
- Goodrich, J.A., Schwartz, M.L. and McClure, W.R. (1990) *Nucleic Acids Res.*, **18**, 4993–5000.
- Grell, K.G. (1973) *Protozoology*. Springer Verlag, New York.
- Hagemann, A.T. and Craig, N.L. (1993) *Genetics*, **133**, 9–16.
- Henikoff, S. (1992) *New Biol.*, **14**, 382–388.
- Herrick, G. (1993) *Semin. Dev. Biol.*, in press.
- Herrick, G., Cartinhour, S., Dawson, D., Ang, D., Sheets, R., Lee, A. and Williams, K. (1985) *Cell*, **43**, 759–768.
- Herrick, G., Cartinhour, S.W., Williams, K.R. and Kotter, K.P. (1987) *J. Protozool.*, **34**, 429–434.
- Hunter, D.J., Williams, K., Cartinhour, K. and Herrick, G. (1989) *Genes Dev.*, **3**, 2101–2112.
- Jaraczewski, J.W. and Jahn, C.L. (1993) *Genes Dev.*, **7**, 95–105.
- Klobutcher, L.A. and Jahn, C.L. (1991) *Curr. Opin. Genet. Dev.*, **1**, 397–403.
- Klobutcher, L.A., Jahn, C.L. and Prescott, D.M. (1984) *Cell*, **36**, 1045–1055.
- Klobutcher, L.A., Turner, L.R. and LaPlante, J. (1993) *Genes Dev.*, **7**, 84–94.
- Mizuuchi, K. (1992) *Annu. Rev. Biochem.*, **61**, 1011–1051.
- Moerman, D.G., Kiff, J.E. and Waterston, R.H. (1991) *Nucleic Acids Res.*, **19**, 5669–5672.
- Plasterk, R.H.A. (1991) *EMBO J.*, **10**, 1919–1925.
- Polard, P., Prere, M.F., Fayet, O. and Chandler, M. (1992) *EMBO J.*, **11**, 5079–5090.
- Prescott, D.M. (1992) *Trends Genet.*, **8**, 439–445.
- Rae, P.P.M. and Spear, B.B. (1978) *Proc. Natl Acad. Sci. USA*, **75**, 4992–4996.
- Rosenzweig, B., Liao, L.W. and Hirsh, D. (1983) *Nucleic Acids Res.*, **11**, 7137–7140.
- Tausta, S.L., Turner, L.R., Buckley, L.K. and Klobutcher, L.A. (1991) *Nucleic Acids Res.*, **19**, 3229–3236.
- Tenzen, T., Matsutani, S. and Ohtsubo, E. (1990) *J. Bacteriol.*, **172**, 3830–3836.
- Williams, K. and Herrick, G. (1991) *Nucleic Acids Res.*, **19**, 4717–4724.
- Yao, M.-C. (1989) In Berg, D.E. and Howe, M.M. (eds), *Mobile DNA*. American Society for Microbiology, Washington, DC, pp. 715–734.

Received on May 11, 1993; revised on August 19, 1993